The 2009 IEEE/RSJ International Conference on
Intelligent Robots and Systems
October 11-15, 2009 St. Louis, USA

Identification of the Servomechanism used for micro-displacement

Ioana-Corina Bogdan and Gabriel Abba

Abstract— **Friction causes important errors in the control of small servomechanism and should be determined with precision in order to increase the system performance. This paper describes the method to identify the model parameters of a small linear drive with ball-screw. Two kinds of friction models will be applied for the servomechanism looking to rise its micro-positioning abilities. The first one includes the static, viscous and Stribeck friction with hysteresis, and the second one uses the Lugre model. The results will be compared taking into account the criterion error, the accuracy and the normalized mean-square-error of the identified mechanical parameters. The coefficients of the models are identified by a recursive identification method using data acquisition and special filtering technics. The least square identification method is used in this paper in order to establish the motor parameters used as initial condition of the recursive estimation method. Computer simulations and experimental results demonstrate the efficiency of the proposed model.**

I. INTRODUCTION

In present miniaturization technology is an important subject in robotics having like objective the obtention of smaller scales for products and devices. Miniaturization is found everywhere starting from convenience goods, electronic products, optical devices, until industrial machines or robots. The manufacturing chains of miniaturized devices demands to industrial machines or robots a high accuracy of micro-displacement, that imply the study of different phenomena. The present work investigates the modeling and the identification of a device used in the electronic industry to make very small core for RFID components. The device use the same technology as in micro-robotics. The realization of these cores need a high precision and a good synchronization between the linear axis displacement and the winding rotation. Our objective is also to obtain a positioning accuracy better than one micrometer and a settling time so short as possible. This objective needs a precise modeling of the axes and more specially the friction occurs during the small displacement.

Friction is a phenomena more or less useful in industrial applications, with undesirable characteristics, generating heat, waste energy, but also positive aspects such as traction or braking [16]. Friction is the result of many physical phenomena, which depends on contact geometry and topology, properties of surface materials of the bodies, displacement and relative velocity of the bodies and the presence of lubrication [10].

Friction represents a nonlinear mechanical phenomenon that is difficult to be completely modeled [5] and the available friction models are empirical, based on limited interpretations and observations, adapted for the specific scope [15].

For ball screw driven servomechanism (BSDS), friction plays an important role being considered a non-linear force that deteriorates the performances of the positioning systems [17] by steady state error, limit cycle or instability [5].

The BSDS may be composed by a servo amplifier, an AC/DC motor, a mechanical drive system (ball-screw, lead-screw or gears), a load, different sensors (encoder, resolver, tachometers or current sensors), and a host controller which generates the motion trajectories [14]. The driving mechanism (ball-screw) and the mechanical structure represent the mechanical subsystem, while the motion generators and the feedback controller with the sensors compose the control subsystem [3].

Friction compensation methods are used to increase the performance of the servomechanisms and to eliminate the friction effects. The high gain feedback, the dither signals or the friction compensation using a controller are reminded in [10] and [18] like solutions that exceed the friction effects. [2] proposed methods which include feedback and feedforward compensation. A feedback or feedforward torque/force loop is given in [4] to compensate the friction using the measured velocity and position. As solution for friction compensation, [19] uses the acceleration feedback which is obtained by differentiating the velocity signal or the acceleration values described by an observer.

Other friction compensation methods were proposed in [3], [5], [6], [11]. In [3], the authors use for friction compensation an identification method in the frequency domain that includes the static, Coulomb, viscous frictions and the Stribeck effect. The parameters estimation is obtained through the limit cycle analysis in velocity feedback loop. For accurate friction identification a Butterworth filter was considered into the velocity feedback loop. [5] use a neural network model in addition with the friction model. [11] proposes a dual speed controller composed by a controller and a friction torque compensator, in order to compensate the nonlinear friction torque. The friction torque compensator adds additional torque corresponding to a nonlinear friction of the mechanical device. Using the same idea, [6] proposes a compensation technique for a positional-dependent friction. The friction function is determined by measuring the static friction in each position.

The authors thank the Council of Region Lorraine, France and the Meusonic company, Marville, France for their financial support.

I.C. Bogdan is with the Department of Design, Manufacturing and Control (LCFC), Paul Verlaine University of Metz, Ile du Saulcy, 57045 Metz Cedex, France bogdanicorina@gmail.com

G. Abba is with the Department of Design, Manufacturing and Control (LCFC), National College of Engineering of Metz, Ile du Saulcy, 57045 Metz Cedex, France abba@univ-metz.fr

The researchers studied and proposed static and dynamic friction models but not for complex systems where external loads appear. The numerical identification of parameters was done for simple systems using the typical friction models [10] (static friction models and dynamic friction models such as Dahl, Lugre, Bliman-Sorine, Armstrong-Helouvry, Reset Integrator, Leuven models).

In this work, we propose to identify the mechanical parameters of the subsystem using friction models described in the second part of the paper. We compare two different models of friction identified with closed-loop simulations using a recursive optimization method. In the same time these results are compared with the least square identification (LSI). The goal of this work is to find the best friction model for a BSDS. The friction model is useful in control systems, for the design of controller or observer in order to compensate the friction effect.

II. MECHANICAL SYSTEM

Our experimental plant consists of two brushless motors coupled with incremental encoders, two positioning controllers from Maxon Motor company, two linear stages (the first one with ball-screw and the second one with compliant nut-screw), an incremental linear encoder and a PC. The resolutions of the angle encoders are 500 impulsions/turn and there are connected to the positioning controllers. The communication for programming and data transfer between positioning controller and the PC is done by a RS-232 serial link. First of all, the study is oriented to the micro-positioning of the ball-screw linear stage. Future works will hint to the comparison of the two linear stages in function of micro-positioning and friction compensation.

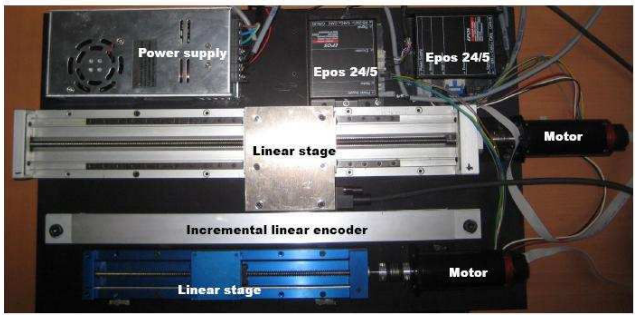

Fig. 1. Two Linear Stage of Experimental Plant

The equations of the behavior of the mechanical subsystem (MSS) are obtained from the motion between the motor and the ball screw driven (BSD):

$$\tau_m = J_m\ddot{\theta}_m + C_m + \tau'_f \tag{1}$$

$$\tau'_f = J_v\ddot{\theta}_s + \tau_f \tag{2}$$

$$\tau_f = F_d\frac{R}{\eta} \tag{3}$$

$$F_d = K_l(\theta_s - \frac{1}{R}x_t) \tag{4}$$

$$F_d = M_t\ddot{x}_t + F_f(\ddot{x}_t, \dot{x}_t, x_t) \tag{5}$$

where τ_m is the motor torque, τ'_f is the torque due to the driving system, τ_f is the load torque on the ball screw, F_d is the driving force, θ_m is the motor position measured by an encoder. The velocity of the motor is noted $\dot{\theta}_m$ and the acceleration $\ddot{\theta}_m$. J_m and J_v are the inertia of the motor shaft and the screw respectively. C_m is the friction torque on the motor and screw side and $F_f(\ddot{x}_t, \dot{x}_t, x_t)$ is the friction force on the sliding table. M_t is the table mass, x_t is the axial position of the table, p is the ball-screw lead, η is the efficiency of the ball-screw, and K_l is the equivalent stiffness coefficient in the axial direction. The coupling between the motor and the BSD has a torsional stiffness coefficient K_θ. The load torque on the ball screw can be calculated by the following equation:

$$\tau_f = K_\theta(\theta_m - \theta_s) \tag{6}$$

The linear to rotational motion factor is represented by a parameter R calculated in function of the lead screw p:

$$R = \frac{p}{2\pi} \tag{7}$$

A modeling of the (MSS) was found in [3]. The MSS being complex, a hypothesis of simplification was adopted: the torsional stiffness coefficient K_θ being very high it is assumed infinite and also the motor position θ_m is supposed to be equal to the screw position $\theta_s = \theta_m$.

The new equations of the MSS are represented by (8) resulted from the replacing of (2) in (1), (3), (4) with the mention that $\dot{\theta}_s$ became $\dot{\theta}_m$ and finally (5).

$$\tau_m = (J_m + J_v)\ddot{\theta}_m + C_m + \tau_f \tag{8}$$

Fig. 2 shows the bloc diagram of the simplified mechanical subsystem (MSS) from the resulted equations.

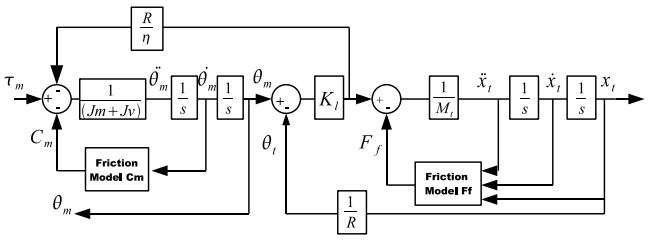

Fig. 2. Mechanical subsystem

Taking into account (1)-(5) and (9)-(13), where the number of unknown parameters was 12, we observe in Fig. 2 that the number of unknown parameters is reduced to 10.

III. FRICTION MODELS

Lots of studies show that friction limits the precision of the positioning systems and arises theirs instability, but for the control applications is needed a simple friction model which captures the essential properties of the friction [20].

In [10], the friction models are classified into two parts: static and dynamic friction models. The simplest friction models found among the static models are the Coulomb and the viscous frictions. Coulomb friction is always present and

opposite to velocity. The magnitude of the Coulomb friction depends on the normal force and the surface properties. Viscous friction corresponds to the lubricated area, and it is proportional to velocity. At zero velocity the viscous friction is zero and for the rest, the friction component increase or decrease with velocity. The lubrication phenomenon can be considered on the basis of the Stribeck effect which is opposite to velocity. The disadvantage of those two friction models is that there are memoryless models that cannot reproduce the stick-slip phenomenon in comparison with some dynamic friction models [20].

The dynamic models capture the presliding phenomenon, the rate dependence and the hysteresis effect. Dahl model is also a simple dynamic model but it cannot predict stick-slip phenomenon, needer the Stribeck effect but it was largely used in engineering. Lugre model which is an extension of Dahl model observes the stick-slip motion and the Stribeck effect [20]. The friction models are empirical, based on interpretations and limitations, and adapted for the servomechanism systems [15] [20].

Friction depends only on velocity for the simplest cases when the friction study is realized for a single rotational axis [1]. When the system contains external loads, the perturbations will deteriorate the servomechanism parameters so that the adopted friction model should be expressed also as a function of position, velocity and for some cases as a function of acceleration [9].

In our paper, there are two friction models considered. One on the motor side expressed by (9) and one on the table side given by (11). We consider only static and viscous frictions on the motor side and a more complex expression function of velocity and acceleration on the table side. For the motor side, the Coulomb friction is represented by F_m and the viscous friction by B_m. On the table side, the Coulomb friction is represented by F_t and the viscous friction by B_t, the Stribeck effect by the terms C_1 and C_2 with V_s the Stribeck velocity. The acceleration $\ddot{\theta}_t$ from the terms C_1 and C_2 permits to introduce an hysteresis effect while the Stribeck effect represented by the exponential term with Vs does not occur during the decreasing phase of the speed, as shown in Fig. 3. The equation (10) defines a fictive rotation angle of the linear displacement of the table.

$$C_m = F_m sign(\dot{\theta}_m) + B_m \dot{\theta}_m \tag{9}$$

$$\theta_t = \frac{x_t}{R} \tag{10}$$

$$F_f = F_t sign(\dot{\theta}_t) + B_t \dot{\theta}_t + C_1 + C_2 \tag{11}$$

where

$$\begin{cases} \text{if } \ddot{\theta}_t > 0 & \text{then } C_1 = C_{s1} \frac{(1+sign(\dot{\theta}_t))}{2} \, e^{-(\frac{\dot{\theta}_t}{V_s})^2} \\ \text{if } \ddot{\theta}_t \leq 0 & \text{then } C_1 = 0 \end{cases} \tag{12}$$

$$\begin{cases} \text{if } \ddot{\theta}_t \geq 0 & \text{then } C_2 = 0 \\ \text{if } \ddot{\theta}_t < 0 & \text{then } C_2 = C_{s2} \frac{(1-sign(\dot{\theta}_t))}{2} \, e^{-(\frac{\dot{\theta}_t}{V_s})^2} \end{cases} \tag{13}$$

Another friction models are chosen in order to make a comparison between our identification results obtained from

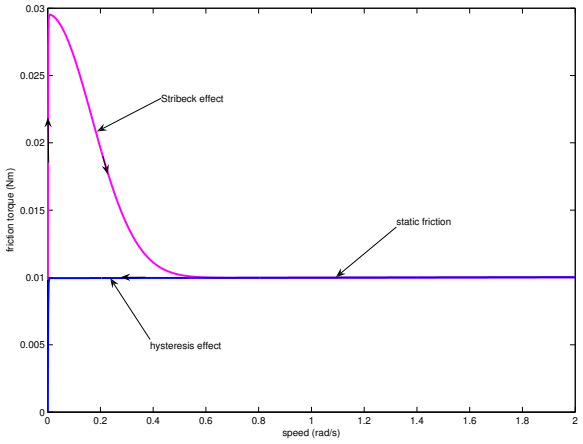

Fig. 3. Friction model with hysteresis

(9) to (13). So for the motor side is considered the simple friction model from (9), and for the table side the Lugre model is applied, that has the ability to capture an internal dynamic of the friction effects.

The Lugre model is expressed by (14) to (16) and described by seven parameters: σ_0 the static friction coefficient, σ_1 the damping coefficient, σ_2 the viscous friction coefficient, V_s the Stribeck effect velocity, z an internal state variable, α_0 the Coulomb friction and the term $(\alpha_0 + \alpha_1)$ represents the stiction force.

$$\frac{dz}{dt} = v - \sigma_0 \frac{|v|}{g(v)} z \tag{14}$$

$$g(v) = \alpha_0 + \alpha_1 e^{-(\frac{v}{V_s})^2} \tag{15}$$

$$F_f = \sigma_0 z + \sigma_1(v) \frac{dz}{dt} + \sigma_2 v \tag{16}$$

The Lugre model is a dynamic model well adapted also for micro-displacements. Eqs. (14) to (16) present the frictional lag in sliding regime, the hysteresis behavior in pre-sliding regime and the break-away force [21].

IV. IDENTIFICATION METHODS

The parameter identification is an experimental technique based on algorithms and procedures that describes a mathematical model of the system using the measured data. The algorithms are classified in non-recursive algorithms which treat the input/output data on a time interval, and recursive algorithms which proceed the input/output data at each moment of time [8]. In our case data acquisition is obtained using an interface provided by the positioning controller, with two sampling periods of $1\,ms$ and $5\,ms$ respectively. The objective is to identify the friction characteristic at the beginning of the displacement. Using a sampling period of $1\,ms$, the identification of inertia terms is more accurate and by $5\,ms$ the friction parameters are more close for the real values.

Because the recorded outputs are noised [7], the signals are treated by applying two successive third order filters. The first one use a classic third order median filter and the second one is a symmetrical non causal mean filter.

The measured data are the actual current value I and the actual position value θ_m. To identify the servomechanism parameters from equations (1) to (13), we need to know the reference position value of the system, the velocity and the acceleration of the motor. The velocity and the acceleration are calculated using a non causal second order derivative filter.

A. Recursive identification method

Fig. 4 shows the algorithm of the recursive identification. The input x is the reference of the system, and the outputs y, $\dot{y}$, $\hat{y}$, $\hat{\dot{y}}$ are the measured position, measured velocity, model estimated position and model estimated velocity respectively.

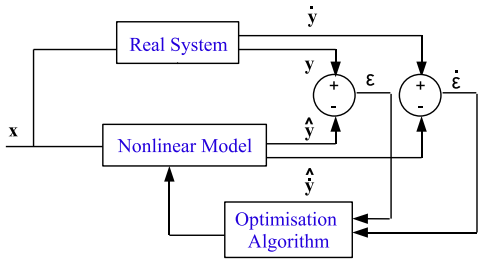

Fig. 4. Recursive identification algorithm

The algorithm try to find a mathematical relation between the outputs and the input which maximize the behavior similitude of the real system and the mathematical model. The algorithm is applied till the square error ε_T is closed by zero. The sensibility method from (17), composed by the position error ε and the velocity error $\dot{\varepsilon}$ gives us:

$$\varepsilon_T = \|y - \hat{y}\| + k\|\dot{y} - \hat{\dot{y}}\| \tag{17}$$

where k is a parameter of convergence. The program is implemented under Matlab. We use the function $fmincon$ to find the minimum of a cost function $\varepsilon_T(\theta)$ which depends on the parameter vector. The solved problems can be written like : $min_\theta\, \varepsilon_T(\theta),\ lb \leq \theta \leq ub$ with an initial condition θ_0 obtained by the least square method and lb and ub are the boundary conditions for the parameter estimation.

An application of this method can be found in [1], where for a close loop system, the two tested friction models (see section 3) are on the table side.

B. Least squares method

The least square method identification (LSMI) gives us the possibility to write the nonlinear equations of the servosystem into a linear way according to the parameters that should be identified [1]. This method can be seen like a method of fitting data. The objective is to adjust in a better way the parameters of a model in manner to fit the data set.

The parameter estimation is obtained solving the new linear equation which minimize the 2-norm of the error. The model of the system must by written as follows:

$$M \cdot \theta = \Psi \tag{18}$$

where Ψ is the output signal, M is the matrix of the measured values and θ is the vector of the unknown parameters.

Applying the LSMI, the vector of the unknown parameters will be computed using (19). In order to obtain an accuracy of θ, the 2-norm condition number of $[M'M]^{-1}$ should be closed to 1.

$$\theta = [M'M]^{-1}M'\Psi \tag{19}$$

According to (18), the non-linear model will be written in a linear form (see (20)).

$$[\ddot{\theta}_m\ \dot{\theta}_m\ sign(\dot{\theta}_m)\ f(\dot{\theta}_m)][J_m B_m F_m C_{s1}]^T = \tau_m \tag{20}$$

where $f(\dot{\theta}_m) = \frac{1+sign(\dot{\theta}_m)}{2}\ e^{-(\frac{\dot{\theta}_m}{V_s})^2}$, J_m is the motor inertia, B_m the viscous friction, F_m the Coulomb friction and C_{s1} the Stribeck effect. The parameter values are given in table I.

While in our test, the velocity is strictly positive, the coefficient C_{s2} can not be identified with the LS-method.

TABLE I
PARAMETER RESULTS WITH LSMI

$J_T = 1.56\ 10^{-5}\ kg\,m^2$	$F_m = 0.01\ Nm$
$B_m = 3.23\ 10^{-5}\ Nm\,s$	$C_{s1} = -0.020\ Nm$

V. CLOSED LOOP IDENTIFICATION

Fig. 5 shows the bloc diagram of the system with the closed loop used for the control. The mechanical subsystem is described in section 2. A PID controller is used to obtain the current reference $\hat{I}$ applied to the power converter. The current of each phases of the brushless motor is controlled by internal loops. The dynamics of these loops can be represented by a first order transfer function with a constant of time T_{ff}. The motor torque is than given by $\frac{K_e}{T_{ff}s+1}\,\hat{I}$. It is imposed a saturation of $[-5\,A, 5\,A]$ for the reference current and a quantization process is applied in order to describe the motor position encoder.

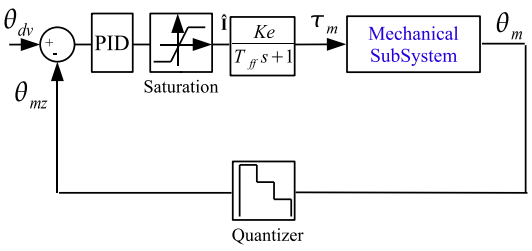

Fig. 5. Close loop simulation model

The same recursive estimation method is applied for parameters identification, with the distinction that the error criterion C_{CL}, the precision parameters P_{CL} and the normalized mean-square-error MSE are calculated by (21), (22) and (23) respectively.

$$C_{CL} = \frac{1}{n}\|I - \hat{I}\| \tag{21}$$

with n the number of data from the vector I.

$$P_{CL} = \frac{\|I - \hat{I}\|}{\|I\|} \tag{22}$$

$$MSE = 100\,\frac{(\|I - \hat{I}\|)^2}{(\|I - mean(I)\|)^2} \tag{23}$$

The normalized MSE indicates a good fit for values between 1% and 5%, and for values less than 1% indicates an excellent fit [7].

TABLE II

PARAMETER RESULTS FOR A SAMPLING PERIOD OF $1\,ms$

Proposed Model	Lugre Model
$J_T = 1.47\ 10^{-5}\ kg\,m^2$	$J_T = 1.46\ 10^{-5}\ kg\,m^2$
$B_m = 0.55\ 10^{-4}\ Nm\,s$	$B_m = 1.04\ 10^{-4} Nm\,s$
$F_m = 6.40\ 10^{-3}\ Nm$	$F_m = 6.11\ 10^{-3} Nm$
$M_t = 481\ g$	$M_t = 440\ g$
$B_t = 4.35\ 10^{-6}\ N\,s/m$	$\sigma_2 = 3.76\ 10^{-6}\ N\,s/m$
$F_t = 15.4\ N$	$\alpha_0 = 8.03\ 10^{-5} N$
$C_{s1} = 3.08\ N$	$\alpha_1 = 7.6\ 10^{-6} N$
$C_{s2} = 0.7\ N$	$V_s = 0.42\ rad/s$
$V_s = 0.43\ rad/s$	$K_l = 2.33\ 10^{-2}\ N/rd$
$K_l = 1.25\ 10^{-2}\ N/rd$	$T_{ff} = 1.39\ 10^{-5}\ s$
$T_{ff} = 1.16\ 10^{-5}\ s$	$\sigma_0 = 1.9\ 10^{-6}\ N/m$
	$\sigma_1 = 3.34\ 10^{-6}\ N\,s/m$

TABLE III

PARAMETER RESULTS FOR A SAMPLING PERIOD OF $5\,ms$

Proposed Model	Lugre Model
$J_T = 1.41\ 10^{-5}\ kg\,m^2$	$J_T = 1.39\ 10^{-5}\ kg\,m^2$
$B_m = 0.61\ 10^{-4}\ Nm\,s$	$B_m = 0.6\ 10^{-4} Nm\,s$
$F_m = 3.52\ 10^{-3}\ Nm$	$F_m = 5.84\ 10^{-3} Nm$
$M_t = 419\ g$	$M_t = 503\ g$
$B_t = 6.34\ 10^{-6}\ N\,s/m$	$\sigma_2 = 4.12\ 10^{-6}\ N\,s/m$
$F_t = 6.03\ N$	$\alpha_0 = 8.58\ 10^{-5} N$
$C_{s1} = 2.32\ N$	$\alpha_1 = 7.89\ 10^{-6} N$
$C_{s2} = 1.7\ N$	$V_s = 0.43\ rad/s$
$V_s = 0.51\ rad/s$	$K_l = 2.51\ 10^{-2}\ N/rd$
$K_l = 3.32\ 10^{-2}\ N/rd$	$T_{ff} = 1.41\ 10^{-5}\ s$
$T_{ff} = 1.48\ 10^{-5}\ s$	$\sigma_0 = 2.13\ 10^{-6}\ N/m$
	$\sigma_1 = 3.28\ 10^{-6}\ N\,s/m$

VI. RESULTS AND COMMENTS

The numerical values of the optimization are shown in II and III for different sampling periods. The left column of the table gives the parameter values of the proposed friction model and the right column gives the parameter values of the Lugre model.

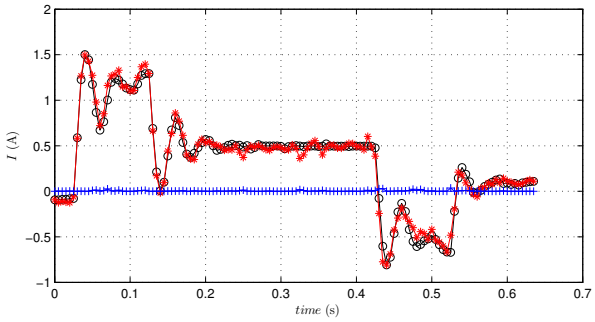

Fig. 6. Comparison between measurement (red) and simulation (black)

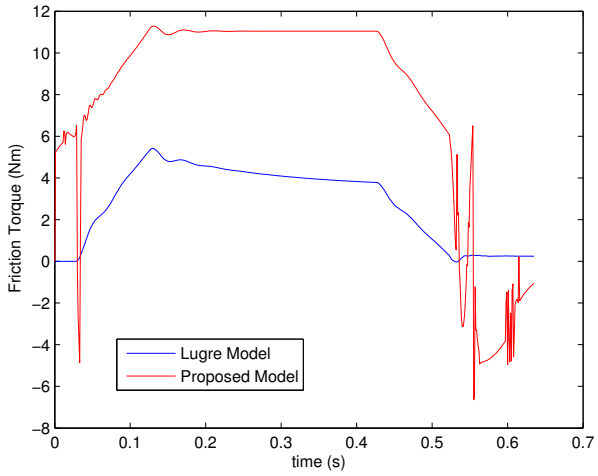

Fig. 7. Comparison of friction torque estimation: proposed model (red) and Lugre model(blue) for the sampling period of $5\,ms$

Fig. 6 indicates that between the measured and estimated current there is a good similarity. The optimum result obtained by simulation with the proposed model is consistent with the measured values. The blue line represents the square of criterion error.

In Fig. 7 is represented the comparison between the friction torque estimations by the proposed model (red) and the Lugre model (blue) respectively. It can be observed that the friction torque obtained by Lugre model is lower that the friction torque resulted from the proposed model. At low speed, the observed switching on the proposed model friction torque is due to the combination of the static friction and Stribeck friction terms.

The only way to determine the friction parameters and show theirs accuracy is to conduct experiments. The friction parameters are very sensitives to vibrations, velocity sliding, temperature, humidity or dust. For our experiments, the chosen velocity is relatively high for about $40\ rad/s$.

The moment of inertia J_T is the sum of the motor shaft and the screw inertia. The results show that for the two set of friction models and for different sampling periods the results are very close and can be compared with the

numerical values provided by the manufacturer. The motor inertia provided by the manufacturer is $1.01\,10^{-5}\ kg\,m^2$. The difference between the two values gives the screw inertia.

The viscous friction values for the motor side and the table side obtained in close loop has small values of $10^{-4}Nm$ and $10^{-6}Nm$ respectively. There are not important influences in the friction force, so these parameters can be neglected.

The Stribeck effect is represented by the term C_{s1} and the Stribeck velocity V_s. The values of V_s are close for the two set of friction models used for the BSDM.

For the proposed model with a sampling period of $5\,ms$ the criterion shows that the error is small, $C_{CL} = 5.4\,mA$ the precision of parameters is around 10% and the normalized mean-square-error is $MSE = 1.43\%$. For the sampling period of $1\,ms$, $C_{CL} = 6.5\,mA$, the precision is 7% and the MSE is 0.60%. The obtained results of the proposed model look more good than the results obtained using the Lugre model, so for the sampling period of $5\,ms$ are $C_{CL} = 5.8\,mA$, $P_{CL} = 11\%$, $MSE = 1.61\%$, and for $1\,ms$ sampling period $C_{CL} = 9.1\,mA$, $P_{CL} = 10\%$ and $MSE = 1.18\%$.

VII. CONCLUSIONS AND FUTURE WORKS

This paper proposes a method to identify the parameters of the model for a mechanical system and more precisely the friction model in order to achieve a good precision of the micro-positioning of the BSDS. The friction model is proposed for mechanical systems that use like load charge on the motor, linear axis with ball-screw or compliant nut-screw transmissions. The mechanical parameters are identified by a recursive identification method which uses data acquisition at different sampling periods. The least square method is used to identify the motor parameters and includes them as initial condition applied in the recursive method. The recursive optimization method is done by a constrained minimization algorithm. In the case of a parameter initialization given by the least square method, the convergence is done with 200 iterative steps. The simulation and the experimental results show that the error in close loop for the proposed friction model and in comparison with the Lugre model is smaller, it has a good accuracy for the identified parameters and the normalized MSE shows a good fit of values for a period of $5\,ms$, and an excellent fit for the period of $1\,ms$. The proposed model encourages future works as the determination of the precision of the parameter estimation, the comparisons of those results with new identification friction models using data obtained from lubricated axes and charging the table with different masses.

REFERENCES

[1] G. Abba, P. Sardain, Modeling of friction in the transmission elements of a robot axis for its identification, *16th IFAC World Congres 2005*, Prague, Czech Republic, July 4–8, Cd ROM 03808.pdf.

[2] B. Armstrong-Helouvry, A survey of models, analysis tools and compensation methods for the control of machines with friction, *Automatica*, vol. 30 (7), pp. 1083–1138, 1994.

[3] M. S. Kim, S. C. Chung, Integrated design methodology of ball-screw driven servomechanisms with discrete controllers. Part 1: Modelling and performance analysis, *Mechatronics*, vol. 16, pp. 491–502, 2006.

[4] E. G. Papadopoulos, G. C. Chasparis, Analysis and model-based control of servomechanism with friction, *Journal of Dynamic Systems, Measurement and Control, Transactions of the ASME*, vol. 126 (4), pp. 911–915, 2002.

[5] S. S. Ge, T. H. Lee, S. X. Ren, Adaptive friction compensation of servomechanism, *International Journal of Systems Science*, vol. 32 (4), pp. 523–532, 2001.

[6] P. Y. Huang, Y. Y. Chen, M. S. Chen, Position-dependent friction compensation for ballscrew table, *Proceedings of the 1998 IEEE International Conference on Control Application*, Trieste, Italy, 1–4 September 1998, pp. 863–867, 1998.

[7] K. Worden, C.X. Wong, U. Parlitz, A. Hornstein, D. Engster, T. Tjahjowidodo, F. Al-Bender, S.D. Fassois, D. Rizos, Identification of pre-sliding and sliding friction, *Mechanical systems and signal Processing*, vol. 21 (1), pp. 514–534, 2006.

[8] I. D. Landau, A. Besancon-Voda, *Identification des systemes*, Edition Hermès, Paris, 2001.

[9] T. S. Kuon, S. K. Sul, H. Nakamura, K. Tsuruta, Identification of the mechanical parameters for servo drive, *Industry Applications Conference, 41st IAS Annual Meeting*. Conference Record of the 2006, vol. 2, pp. 905–910, 2006.

[10] H. Olsson, H. J. Astrom, C. Canudas de Wit, M. P. Gafvert, Friction models and friction compensation, *IEEE/RSJ International Conference on Intelligent Robots and System, IROS'02*, vol. 3, pp. 2109–2114, 2002.

[11] D. H. Lee, J. W. Ahn, Dual speed control scheme of servo drive system for a nonlinear friction compensation, *IEEE Transaction on Power Electronics*, vol. 23 (2), pp. 959–965, 2008.

[12] M. S. Kim, S. C. Chung, Friction identification of ball-srew driven servosystems through the limit cycle analysis, Intelligent Robots and System, *Mechatronics*, vol. 16, pp. 131-140, 2006.

[13] P. I. Ro, W. Shim, S. Jeong, Robust friction compensation for submicrometer positioning and traking for a ball-screw-driven slide system, *Precision Enginnering*, vol. 24, pp. 160-173, 2000.

[14] Ying-Yu Tzou, S. Jeong, Introduction to servo system design, *Institute of Control Engineering, National Chiao Tung University*, http://pemclab.cn.nctu.edu.tw, 1997.

[15] F. Al-Bender, J. Swevers, Characterisation of friction force dynamics, Behaviour on modeling and macro scales, *IEEE Control Systems Magasine*, vol. 28 (6), pp 64–81, December 2008.

[16] A. Harnoy, B. Friedland, S. Cohn, Modeling and measuring friction effects, *IEEE Control Systems Magasine*, vol. 28 (6), pp. 82-91, December 2008.

[17] K. Sato, Trend of precision positioning technology, *18th International Congress of Mechanical Engineering, Proceedings of COBEM 2005*, November 6–11, 2005, Ouro Preto, Brasilia.

[18] B. de Jager, Iproving the tracking performance of mechanical systems by adaptive extended friction compensation, *IFAC 12th Triennial World Congress*, Sydney, Australia, vol. 3, pp. 109–114, 1993.

[19] D. Stajik, N. Peric, J. Deur, Friction compensation methods in position and speed control systems, *Proceedings of the IEEE International Symposium on Industrial Electronics*, Slovenia, vol. 3, pp. 1261–1266, 1999.

[20] K. J. Astrom, C. Canudas de Wit, Revisiting the LuGre friction model, Stick-slip motion and rate dependence, *IEEE Control Systems Magasine*, vol. 28 (6), pp. 101-114, December 2008.

[21] V. Lampaert,J. Swevers, F. Al-bender, Experimental comparison of different friction models accurate low-velocity tracking, *Proceeding of the 2004 American Control Conference*, Boston, Massachusetts, June 30–July 2, vol.2, pp. 1121–1126, 2004.